Enhancement of Birefringence using Metal-filled Suspended Core Microstructured Optical Fibers

Rajat Kumar Basak[1,2], Debashri Ghosh[1]
1. Fiber Optics and Photonics Division, CSIR-Central Glass and Ceramic Research Institute, Kolkata-700032, WB, India.
2. School of Material Science and Nanotechnology, Jadavpur University, Kolkata-700032, WB, India.

Abstract: We present the utilization of RF module of COMSOL Multiphysics that implements the finite element method (FEM) for 2D mode analysis of our proposed metal-filled suspended core microstructured optical fiber (SC-MOF) structures. Mode analysis helps to study the fiber properties and investigate the possibility of enhancement of birefringence. The interaction between the core-guided light and metal is increased due to the suspended core structure eventually leading to enhancement of surface plasmon polariton (SPP) coupling and surface plasmon resonance (SPR). By taking Sellmeier's equation and Lorentz-Drude model into account, effective indices of fundamental modes are determined for the required wavelength range. Birefringence is determined from the index difference of the two orthogonally polarized fundamental modes and its variation is studied as a function of wavelength for various SC-MOF designs. This study is important for designing polarization-maintaining (PM) fibers with improved performance and SC-MOF based in-fiber polarizers for a particular wavelength range.

Keywords: birefringence, suspended core microstructured optical fibers, suspension factor, surface plasmon resonance.

1. Introduction

A microstructured optical fiber (MOF) [1] consists of a solid silica core surrounded by a hexagonal lattice of microscopic air holes running along the entire fiber length and guides light by modified total internal reflection (M-TIR). Compared to the conventional optical fibers, MOFs offer some unique properties like endlessly single mode behaviour, high birefringence, novel dispersion properties, etc. and also provide extra freedom in tailoring the fiber properties by suitably tuning the geometrical parameters. The hole diameter (d), pitch (distance between two adjacent air holes denoted by ş) as well as their ratio (d/ş) play a vital role in designing any MOF structure.

In the twenty first century, surface plasmon resonance (SPR) has attracted much research attention around the globe. It is basically a near-field electromagnetic phenomenon that develops around the surface area of a metal-dielectric interface. When the light waves (consisting of photons) are incident on the metal-dielectric interface, oscillations of the free electrons occur on the metal surface and the light waves couple to the free electrons, hence forming surface plasmons in that region. The resonance condition occurs when the frequency of the incident light wave and the electron oscillation frequency are consistent. In this condition, the energy of the electromagnetic field is transformed into the free electron oscillation energy, which helps to develop a special form of electromagnetic mode. This newly developed electromagnetic mode, known as surface plasmon polariton (SPP), is enhanced and confined around the metal surface when phase-matching condition is satisfied thus leading to surface plasmon resonance (SPR). In a plasmonic MOF, SPPs are formed around the surface of the metal-filled hole. When the phase matching condition is satisfied, the core guided light can be strongly coupled with the generated SPP, which has been extensively studied [2,3]. Coupling of core guided light with SPP modes at particular SPR wavelengths implies potential applications in fiber based optical filtering, sensing, nonlinear optics, etc.

In this paper, we have shown the enhancement of birefringence of the proposed SC-MOF structures with metal-filled air hole in the cladding. These SC-MOFs were designed using COMSOL Multiphysics (version 4.3b) and their modal properties were studied. The results show improvement in birefringence with increase in suspension factor (SF) for a fixed pitch. The birefringence value reported in this work is an order of magnitude higher than that achieved in commercial PM fibers.

2. Structure of the Proposed SC-MOFs and Fundamental Theory

In this work, our proposed SC-MOFs with hexagonal lattice arrangement of air holes have ع = 2 µm and d/ع = 0.95. In the case of SC-MOFs, the air holes in the first ring of the cladding are elongated and tapered towards the center of the core, which can be controlled by a geometrical parameter known as suspension factor (SF). The allowable range of SF for a specific MOF structure is restricted by the geometrical parameters d and ş .

We have considered the maximum and minimum values of SF based on the study given in [4] and have implemented them accordingly in this work. For theoretical analysis of the SC-MOF designs using COMSOL Multiphysics, each air hole present in the first ring is formed by a combination of a circle and a second order Bézier curve [5], which is basically the path traced by the function B(t), defined by equation (1) [6],

$$B(t) = (1-t^2)P_1 + 2(1-t)tP_2 + t^2P_3 \quad t \in (0,1) \qquad (1)$$

Here, P_1, P_2 and P_3 are the three control points and t is the varying parameter. Formation of such a Bézier curve and an air hole adjacent to the core in a SC-MOF is schematically depicted in Figure 1 (a) and (b), where the centre of the circular air hole and the centre of the entire MOF geometry are denoted by O and C respectively in (b).

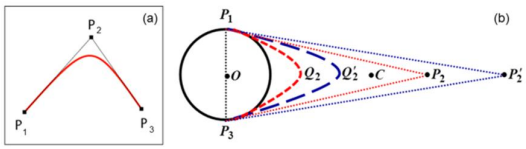

Figure 1. Schematic diagram of the (a) second order Bézier curve; (b) elongated air hole formed by the combination of a circle and Bézier curve.

The SF of a SC-MOF can be defined as OP_2/OC and different suspension conditions can be achieved by manipulating the control point P_2 of the Bézier curve, shown in Fig. 1. For example, the point P_2^{α} denotes a different position of P_2, thereby generating a different Bézier curve, $P_1Q_2^{\alpha}P_3$ that ultimately leads to a change in the SF than that obtained by $P_1Q_2P_3$. A suspended core structure is schematically represented in Figure 2 [4], [7]. It is to be noted that the SF cannot possess any arbitrary value and is delimited by an upper and lower value due to structural integrity. The lowest value of SF corresponds to an ideal circular structure and the value can be increased till the point the holes maintain their individuality and do not merge with each other.

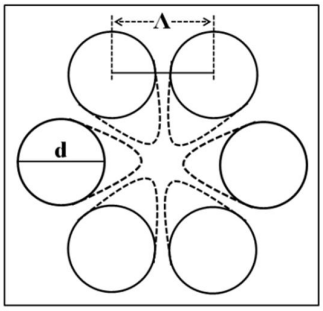

Figure 2. Schematic representation of the difference between the first ring of an ideal circular MOF and a SC-MOF in which the elongated air hole is formed by a combination of a circle and second order Bézier curve.

Based on the relations suggested in [4] and also shown in equation (2) for calculating the maximum (SF_{max}) and minimum (SF_{min}) values of SF, the possible values of SF for d/ş = 0.95 were determined.

$$SF_{min} = \frac{d}{\Lambda}; \quad SF_{max} = 2.5 - \frac{d}{\Lambda} \qquad (2)$$

For our proposed SC-MOF designs, the SF value lies within the range 0.95 Ò SF Ò 1.55, from which we select SF = 0.95 (SF_{min}), 1.15, 1.35 and 1.55 (SF_{max}) for our study. The cross-sections of the proposed SC-MOF structures are drawn in the 'Geometry' section of COMSOL Multiphysics using circles and quadratic Bézier polygon with specific control points for denoting different SFs and are shown in Figure 3.

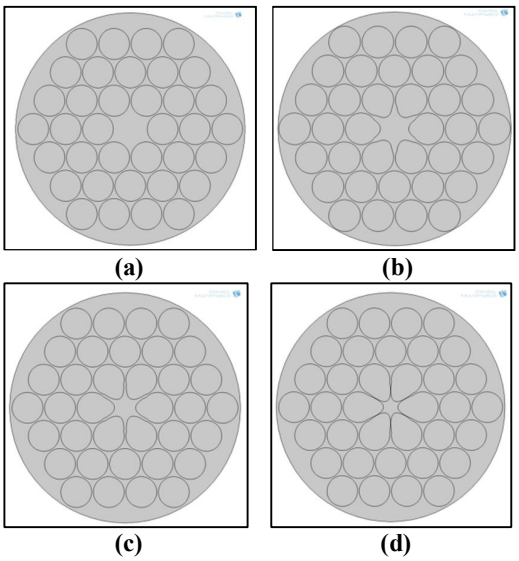

Figure 3. Cross sections of SC-MOF designs in COMSOL GUI having d/ş = 0.95, ş = 2 εm, and different SF values of (a) 0.95 (perfectly circular), (b) 1.15, (c) 1.35 and (b) 1.55.

For all the SC-MOF designs, pure silica is used as the core and matrix material and its refractive index n(∂) is calculated in COMSOL Multiphysics by incorporating the Sellmeier's equation [8] as follows,

$$n(\lambda) = C_0 + C_1\lambda^2 + C_2\lambda^4 + \frac{C_3}{(\lambda^2 - l)} + \frac{C_4}{(\lambda^2 - l)^2} + \frac{C_5}{(\lambda^2 - l)^3} \qquad (3)$$

where,
C_0= 1.4508554, C_1= -0.0031268, C_2= -0.0000381, C_3= 0.0030270, C_4= -0.0000779, C_5= 0.0000018 and l = 0.035.

We have used gold (Au) to fill one air hole along the horizontal direction in the first ring of our proposed SC-MOF designs as shown in Figure 4. The permittivity and hence the frequency dependent refractive index of gold is calculated by using the Lorentz-Drude (LD) model [9] and the expression is given by equation (4),

$$\varepsilon(\omega) = \varepsilon_{\infty} - \frac{\omega_p^2}{\omega(\omega + j\Gamma)} + \sum_{i=1}^{M} \frac{f_i \omega_p^2}{\omega_i^2 - \omega^2 - j\omega\Gamma_i} \quad (4)$$

where ε_∞ represents the dielectric constant at infinite frequency (considered as 1), ω_p represents the plasma frequency of the electron gas, M is the number of oscillators having frequency ω_i, strength f_i and life time $1/\Gamma_i$.

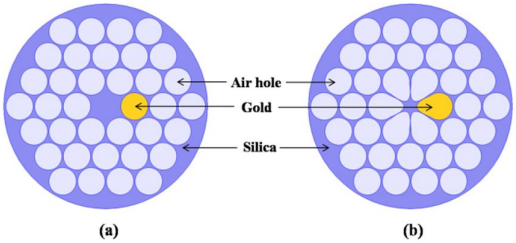

Figure 4. Schematic representation of metal-filled SC-MOF with (a) SF_{min} = 0.95 (circular air holes) and (b) SF_{max} = 1.55. The blue region represents silica, yellow and white circles represent gold-filled and air-filled holes respectively.

In the COMSOL analysis, both Sellmeier's equation and LD model are incorporated by specifying the parameters under 'Global definitions' and variables under 'Model (Definitions)'. Material properties in terms of refractive index are then assigned to the respective domains in the 'Materials' section. In the next step, the entire MOF structure is divided into minute triangular elements using 'Physics-controlled Mesh', which is shown in Figure 5. For all the designs considered in this work, the size of the mesh is optimized and 'Extremely fine' is the chosen mesh size. Finally, the complex effective indices of the fundamental modes are determined for the required wavelength range using a 'Parametric Sweep'.

The absorption loss (in dB/m) for the proposed SC-MOF designs is calculated using equation (5),

$$\alpha = \frac{20}{\ln(10)} \frac{2\pi}{\lambda} \mathrm{Im}\left(n_{eff}\right) \times 10^6 \quad (5)$$

where $\mathrm{Im}(n_{eff})$ indicates the imaginary part of the effective index and λ denotes the operating wavelength.

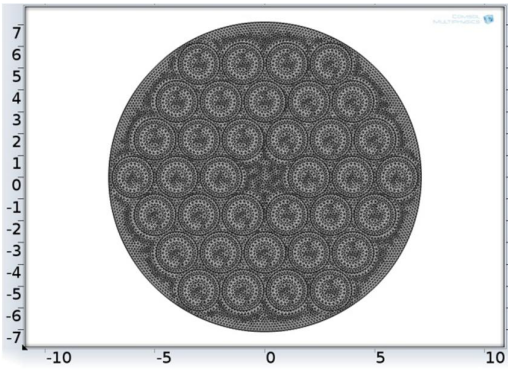

(a)

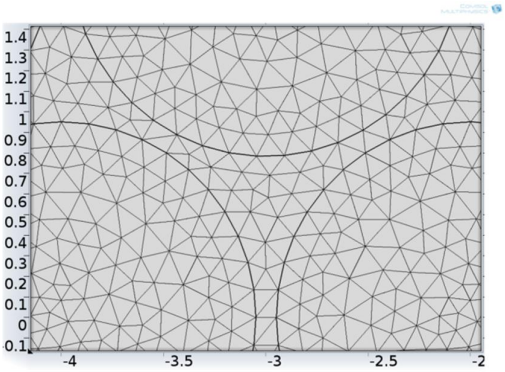

(b)

Figure 5. (a) Schematic representation of physics-controlled mesh applied in a MOF structure, and (b) its magnified view in COMSOL GUI.

3. Simulation Results and Analysis

RF module of COMSOL Multiphysics was used for '2D Mode Analysis' in the 'Frequency Domain' of the proposed SC-MOFs. By taking Sellmeier's equation and LD model into account, modal characteristics of our fiber designs are studied numerically. We have analysed the dispersion properties and the modal profiles of the x-polarized and y-polarized fundamental core-guided modes for the four SC-MOF structures. The dispersion and loss curves of the fundamental mode for both x and y-polarization are shown in Figure 6 and Figure 7 respectively. We find that the x-polarized mode couples more strongly with the SPP mode than the y-polarized mode.

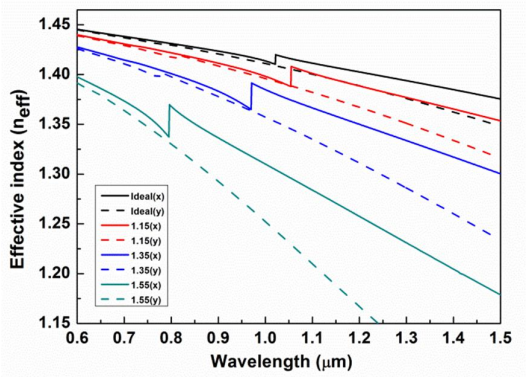

Figure 6. Dispersion curves of x-polarization (solid curves) and y-polarization (dashed curves) of a gold-filled SC-MOF having d/ş = 0.95, ş = 2 εm and SF = 0.95 (black lines), 1.15 (red lines), 1.35 (blue lines) and 1.55 (green lines).

From the dispersion curves in Figure 6, it is clearly seen that the dispersion curves split into two branches at the complete coupling regions. At the point of discontinuity, the upper and lower branch modes contain dissimilar values of effective index (n_{eff}) and closely equal (not exactly) loss values that

give rise to the complete coupling phenomenon. But in the case of incomplete coupling, these curves are continuous. The corresponding SPP mode and the core-guided mode have almost equal value of n_{eff} in the case of incomplete coupling while their loss values differ by a huge margin.

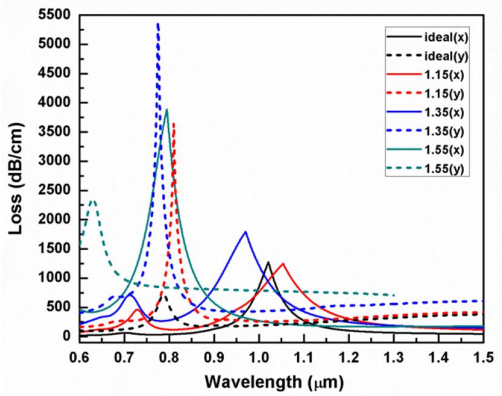

Figure 7. Loss curves of x-polarization (solid curves) and y-polarization (dashed curves) of a gold-filled SC-MOF having d/ş = 0.95, ş = 2 ε m and SF = 0.95 (black lines), 1.15 (red lines), 1.35 (blue lines) and 1.55 (green lines).

For SF = 0.95 (ideal), complete and incomplete SPP coupling occurs at the surface plasmon resonance (SPR) wavelength of 1.021 μm and 0.704 μm respectively for x-polarization, but for y-polarization, only incomplete coupling occurs at 0.787 μm and no complete coupling occurs. For SF = 1.15, complete and incomplete SPP coupling occurs along x-polarization at the SPR wavelength of 1.054 μm and 0.729 μm and at 0.81 μm and 0.7 μm along y-polarization respectively. For SF = 1.35, the same occurs at the SPR wavelength of 0.97 μm and 0.712 μm respectively for x-polarization and at 0.776 μm and 0.681 μm respectively for y-polarization. Finally for SF = 1.55 a complete SPP coupling was observed at 0.795 μm. For y-polarization, we could not find any complete coupling, but an incomplete coupling point was observed at 0.630 μm. Modal profiles corresponding to SF = 1.35 and 1.55 for x-polarization at the complete and incomplete coupling regions are shown in Figure 8.

Due to high d/ş value as well as increase in SF values, the silica core becomes smaller and tightly bounded by the first ring of the SC-MOF. This leads to enhanced interaction of the core guided light with the surrounding air holes. Hence the horizontally placed gold-filled air hole in the first ring absorbs maximum energy of the transmitted light, which leads to the strong SPP coupling along horizontal direction and less energy absorption along vertical direction. Due to this reason, no complete coupling region occurs for the highest SF along y-polarization.

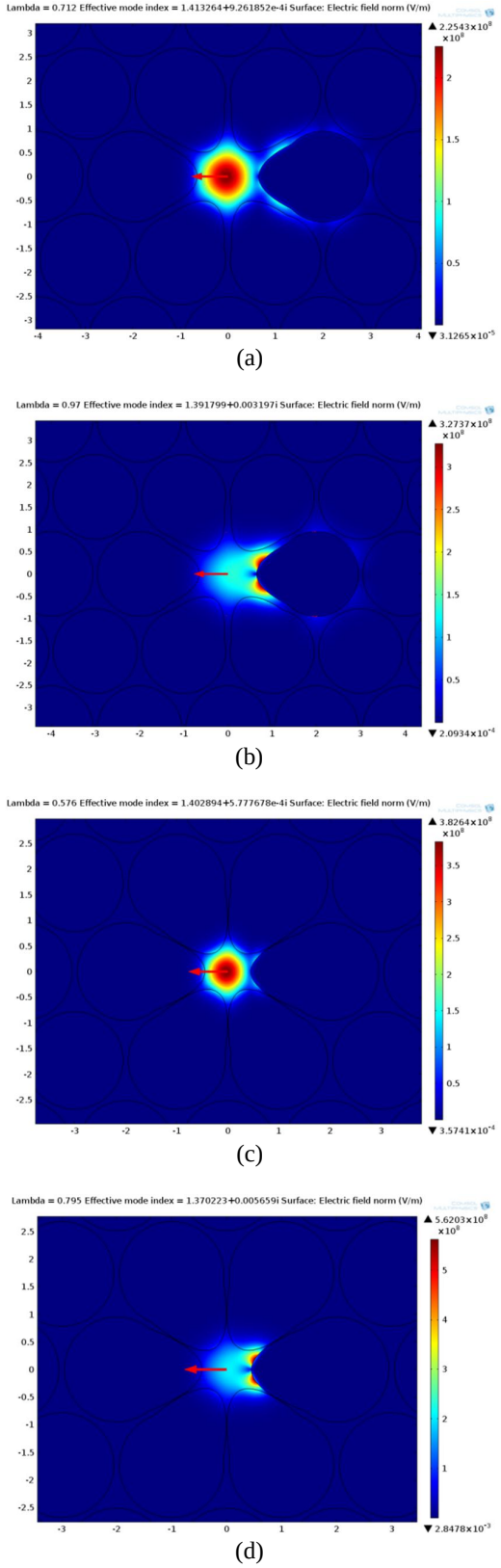

Figure 8. Modal profiles of the fundamental mode along x-polarization of the proposed SC-MOF for SF = 1.35 (a & b) and 1.55 (c & d) showing incomplete (a & c) and complete (b & d) coupling phenomenon.

From Figure 6, it can be noted that the difference between the two orthogonally polarized modes (i.e. x and y-polarized modes) is increased with the increase in SF values towards higher wavelength regime. This effective index difference between the two orthogonally polarized modes is defined as the modal birefringence (B), which can be expressed by the following relation,

$$B = \Delta n_{eff} = \left| n_x - n_y \right| \quad (6)$$

where the effective indices of the x and y-polarized modes are denoted by n_x and n_y respectively. By using the above relation, we have calculated the birefringence for each SF value, and it is graphically represented in Figure 9.

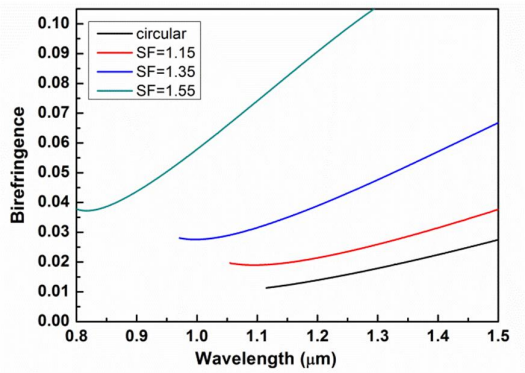

Figure 9. Variation of birefringence with wavelength for the gold-filled SC-MOF designs having d/ş = 0.95, ş = 2 εm and SF = 0.95 (black lines), 1.15 (red lines), 1.35 (blue lines) and 1.55 (green lines).

Improvement in modal birefringence for higher wavelength is an obvious outcome which is already seen in Figure 6. Along with it, our study also clearly shows the enhancement of modal birefringence with increasing SF values. For maximum SF (i.e. 1.55), the birefringence value is 0.126 at the wavelength of 1.50 μm which is an order of magnitude higher than the existing birefringent fibers.

4. Conclusions

In the present work, enhancement of modal birefringence is obtained by using a novel design of gold-filled SC-MOF. We use the RF module of COMSOL Multiphysics software to analyze the dispersion properties and modal profiles of the SPP coupled core-guided modes of our proposed SC-MOFs. Numerical results show that the modal birefringence is increased with increasing SF values and for the maximum SF i.e. SF = 1.55, at wavelengths beyond 1 εm, it is increased by an order of magnitude compared to the birefringence of the existing commercial fibers. Hence these SC-MOFs have the potential of efficiently functioning as PM fibers with improved performance or in-fiber polarizers for a particular wavelength range.

References

1. P. St. J. Russell, ôPhotonic-crystal fibers,ô *J. Ligthwave Technology*, **24** (12), 4729-4749 (2006).
2. A. Nagasaki, K. Saitoh and M. Koshiba, 'Polarization characteristics of photonic crystal fibers selectively filled with metal wires into cladding air holes,' *Optics Express*, **19** (4), 3799-3808 (2011).
3. G. An, S. Li, X. Yan, Z. Yuan and X. Zhang, 'High-birefringence photonic crystal fiber polarization filter based on surface plasmon resonance,' *Applied Optics*, **55** (6), 1262-1266 (2016).
4. D. Ghosh, S. Bose, S. Roy and S. K. Bhadra, 'Design and fabrication of microstructured optical fibers with optimized core suspension for enhanced supercontinuum generation,' *J. Lightwave Technology*, **33** (19), 4156-4162 (2005).
5. G. Farin, *Curves and surfaces for Computer Aided Geometric Design*, 57-93, Academic Press, USA (2002).
6. K. M. Mohsin, M. S. Alam, D. M. N. Hasan and M. N. Hossain, 'Dispersion and nonlinearity properties of a chalcogenide As_2Se_3 suspended core fiber,' *Applied Optics*, **50** (25), 102-107 (2011).
7. D. Ghosh, S. Roy and S. K. Bhadra, ôEfficient supercontinuum sources based on suspended core microstructured fibers,ô *IEEE Journal of Selected Topics in Quantum electronics*, **20** (5), 597-604 (2014).
8. Ajoy Ghatak and K. Thyagarajan, *Introduction to fiber optics*, 80-83, Cambridge University Press (2011).
9. A. D. RakiĆ, A. B. DjuriĦ, J. M. Elazar and M. L. Majewski, ôOptical properties of metallic films for vertical-cavity optoelectronic devices,ô *Applied Optics*, **37** (22), 5271-5283 (1998).

Acknowledgements

Authors would like to thank the Director, CSIR-CGCRI, Kolkata, HoD, Fiber Optics and Photonics Division, CSIR-CGCRI, Kolkata and the Director, School of Material Science and Nanotechnology, Jadavpur University, Kolkata.